Biomed Microdevices (2009) 11:103–115
DOI 10.1007/s10544-008-9214-3

Biomimetic hydrogels for biosensor implant biocompatibility: electrochemical characterization using micro-disc electrode arrays (MDEAs)

Gusphyl Justin · Stephen Finley · Abdur Rub Abdur Rahman · Anthony Guiseppi-Elie

Published online: 5 August 2008

Abstract Our interest is in the development of engineered microdevices for continuous remote monitoring of intramuscular lactate, glucose, pH and temperature during post-traumatic hemorrhaging. Two important design considerations in the development of such devices for in vivo diagnostics are discussed; the utility of micro-disc electrode arrays (MDEAs) for electrochemical biosensing and the application of biomimetic, bioactive poly(HEMA)-based hydrogel composites for implant biocompatibility. A poly(HEMA)-based hydrogel membrane containing polyethylene glycol (PEG) was UV cross-linked with tetraethyleneglycol diacrylate following application to MDEAs (50 μm discs) and to 250 μm diameter gold electrodes within 8-well culture ware. Cyclic voltammetry (CV) of the MDEAs revealed a reduction in the apparent diffusion coefficient of ferrocenemonocarboxylic acid ($FcCO_2H$), from 6.68×10^{-5} to 6.74×10^{-6} cm^2/s for the uncoated and 6 μm thick hydrogel coated devices, respectively. Single frequency (4 kHz) temporal impedance measurements of the hydrogels in the 8-well culture ware showed a reversible 5% change in the absolute impedance of the hydrogels when exposed to a pH change between 6.1 to 7.2 and a 20% drop between pH 6.1 and 8.8.

Keywords Biotransducers · Implantable biosensors · Integrated circuits · Arrays · Electroanalysis

G. Justin · S. Finley · A. R. Abdur Rahman · A. Guiseppi-Elie (✉)
Center for Bioelectronics, Biosensors and Biochips (C3B), Clemson University Advanced Materials Center, 100 Technology Drive, Anderson, SC 29625, USA
e-mail: guiseppi@clemson.edu

G. Justin
e-mail: gusphyl@clemson.edu

S. Finley
e-mail: sfinley@clemson.edu

A. R. Abdur Rahman
e-mail: abdur@clemson.edu

S. Finley · A. Guiseppi-Elie
Department of Chemical and Biomolecular Engineering, Clemson University, Clemson, SC 29634, USA

A. Guiseppi-Elie
Department of Bioengineering, Clemson University, Clemson, SC 29634, USA

1 Introduction

This paper addresses the synthesis and characterization of a biomimetic hydrogel that serves as the responsive and encapsulating membrane for an implantable amperometric biotransducer (based on enzyme activity) useful for the continuous *in vivo* monitoring of glucose and lactate (Abraham et al. 2005). *In vivo* electrochemical biosensors are promising tools for clinical applications involving real time medical diagnostics linked to therapeutic intervention (Wilson and Gifford 2005; Murphy 2006). There is a wealth of published literature on amperometric biosensors for both *in vivo* and *in vitro* glucose monitoring (Moussy et al. 1993; Moser et al. 2002; Ward et al. 2004; Schuvailo et al. 2006; Yu et al. 2007). The feasibility of developing an implantable, dual sensing, glucose and lactate amperometric enzyme biosensor as the responsive biotransducer to a fully integrated wireless biochip has previously been introduced (Guiseppi-Elie et al. 2005; Farahi et al. 2007). The measurement of physiologic lactate concentrations is of particular interest because its temporal variation can provide an indication of the extent and severity of

hemorrhage associated with traumatic injury (Vincent 1998; Ward et al. 2001). Following injury that results in tissue hypoxia; interstitial lactate levels rise and are the main source of metabolically produced acid responsible for tissue acidosis. Since lactate and glucose exist in equilibrium between the interstitial and vascular compartments, interstitial concentrations of these metabolites should thus be reflective of their systemic levels.

The ability to monitor *in vivo* lactate, along with glucose, in the interstitium is possible but current methods are either not clinically feasible for prolonged periods of measurement or are unreliable because they suffer from the deleterious effects of endogenous interferences, fouling and eventual fibrous encapsulation (Pickup et al. 1993; Moussy et al. 1994; Gerritsen et al. 2000; Gifford et al. 2006). The application of a biocompatible and biomimetic hydrogel layer to the surface of a glucose-lactate sensing biochip may serve as a means of reducing the host foreign body response, as well as to maintain the bioactivity of immobilized enzymes. Our goal is to develop an implantable lactate and glucose sensing biochip for temporary intramuscular implantation that is capable of telemetered reporting of local lactate and glucose levels in the battlefield for wounded military and civilian trauma victims.

The design of an implantable, enzyme-based, electrochemical biotransducer should take into consideration the following criteria: (1) adequate mass transport of the analyte to the electrode surface; (2) rapid electron transfer kinetics; (3) stability of the immobilized enzyme; (4) isolation of the stabilized enzyme from host protease activity and (5) biocompatibility. Hydrogel membrane layers serve as effective micro-bioreactors for the stabilization of bioactive entities such as enzymes (Steinschaden et al. 1997). Moreover, hydrogels have an extensive history of successful biomedical use, such as in contact lenses (Holly and Refojo 1975). The release of anti-inflammatory agents and growth factors to address the early stages of the pro-inflammatory host response may also be useful adjuvants enabled by the use of hydrogels (Bhardwaj et al. 2007). However, successful integration of these hydrogel membrane layers with underlying microelectrode structures depends upon proper characterization of ion and small molecule transport through these hydrogel layers.

Different microelectrode geometries have been proposed and investigated; amongst these are micro-discs (Davies et al. 2005), micro-bands (Compton et al. 1993), micro-squares (Morita et al. 1988) and interdigitated micro-electrodes (Morita et al. 1997). For adequate mass transport through hydrogel layers, micro-disc electrode arrays (MDEA) have been proposed by Guiseppi et al. (2005) (Guiseppi-Elie et al. 2005) and in recent years MDEAs have been extensively studied by experimental (Davies et al. 2005) and simulation techniques (Davies and Compton 2005; Lee et al. 2001). Davies et al. reported on a two-dimensional simulation method for the cyclic and linear sweep voltammetric response of micro-disc arrays (Davies and Compton 2005), while Lee et al. (2001) reported on a three-dimensional simulation method. Gonzalez-Garcia et al. (2007) characterized some prototypes of gold ultramicroelectrodes (UMEs) using voltammetry and chronoamperometry. Based on these previous studies, as the time scale of the voltammetric experiment increases, the current response of the micro-disc array can be found to cover four distinct diffusional domains (Davies and Compton 2005): (1) at short times, MDEAs or UMEs work individually and are controlled by linear diffusion, (2) at larger times, arrays reach *the steady-state current controlled by radial diffusion*, (3) at still longer times the diffusion layers overlap and the disc arrays stop working as separate electrodes, (4) finally, complete overlapping diffusion fields occur and the micro-disc array behaves like a macroelectrode under the control of semi-infinite linear diffusion. This is schematically illustrated in Fig. 1.

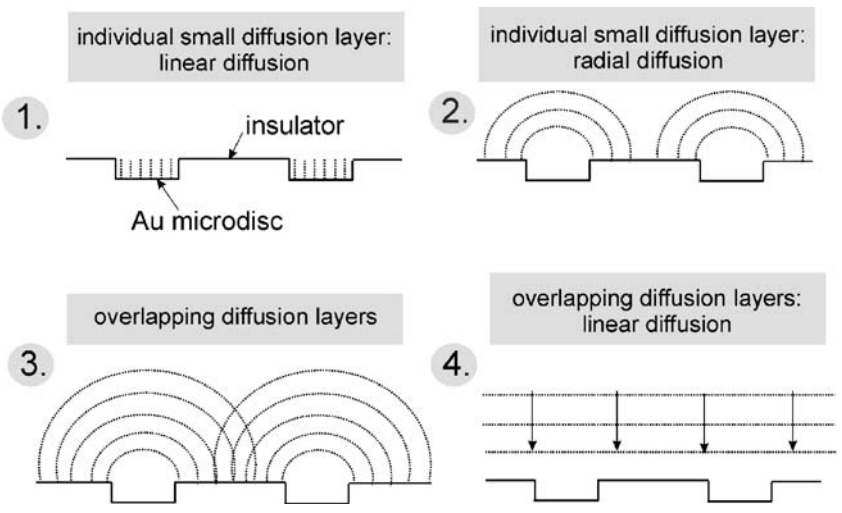

Fig. 1 Schematic diagram illustrating the four generalized categories of diffusion profile that may develop for an array of micro-disc electrodes

For bioanalytical biotransducer applications involving an enzyme-containing hydrogel layer, one key design issue is to match the transport characteristics of the hydrogel layer and the immobilized enzyme activity with the overall geometric parameters of the device, including thickness of the hydrogel layer, size and inter-disc spacing of the micro-disc array and density of the micro-discs. The design goal is to achieve low background current (Faradaic and charging), low signal-to-noise, improved sensitivity, lower limits of detection and impedance matching with the intended potentiostat electronics while maintaining the smallest possible implant dimensions. This paper reports on the behavior of hydrogel layers at three gold micro-disc array electrodes. The first is the MDEA 050-Au, a 1.0×2.0×0.05 cm chip with an electrochemically active gold surface area of 0.1 cm^2 that may be routinely handled in the laboratory. The second is the ECC MDEA 5037-Au, a 4.0×2.0 mm×0.05 cm chip with an electrochemically active gold surface area of 7×10^{-4} cm^2 that is designed and packaged for animal implantation. The third is a 250 μm diameter gold microelectrode formed at the bottom of an eight-well cell culture ware. Both MDEA chips were designed with working electrodes that are formed from a single contiguous layer of gold that sits beneath a hexagonal close packed array of 50 μm diameter windows formed through a 0.5 μm thick silicon nitride (Si_3N_4) layer. Hydrogel layers on these electrodes were formed from poly(hydroxyethyl methacrylate) {(p(HEMA)} synthesized from tetraethyleneglycol diacrylate (TEGDA) cross-linked HEMA, poly(ethyleneglycol(200))methacrylate (PEG(200)MA) and [tris(hydroxymethyl)methyl]- acrylamide (HMMA)}.

Electrochemical techniques were used to elucidate; (1) the effect of the hydrogel sensing layer on diffusion of electroactive species to the MDEA devices, and (2) the interfacial impedance changes associated with application of the hydrogel biorecognition layer. Cyclic voltammetry (Nicholson and Shain 1964; Finklea et al. 1993; Bard and Faulkner 2001) and AC electrical impedance spectroscopy (EIS) (Finklea et al. 1993) of a Tris buffer solution of ferrocene monocarboxylic acid ($FcCO_2H$) were carried out at hydrogel-coated and uncoated MDEAs in an effort to characterize mass transport of the ferrocene electron mediator within the hydrogel layer as well as to evaluate the capacitative and charge transfer characteristics at the electrode-solution and electrode-hydrogel interfaces. The effect of variable pH (6.1 to 8.8) on the impedance characteristics of the hydrogel was also investigated using single frequency temporal impedance analysis (EIA) in an effort to evaluate not only how the amperometric response of the biochip would vary with acidosis, but also how the impedance property of the system would change within a dynamic physiological environment.

2 Experimental

2.1 Materials

2.1.1 Reagents

Hydroxyethylmethacrylate (HEMA), tetraethyleneglycol diacrylate (TEGDA, technical grade), *N*-[tris(hydroxymethyl) methyl]-acrylamide, (HMMA, 93%), 2,2-dimethoxy-2-phenylacetophenone (DMPA, 99%), (3-aminopropyl)trimethoxysilane (γ-APS, 97%), 3-mercapto-1-propanol (95%) were purchased from Sigma-Aldrich Co. (St. Louis, MO, USA). Poly(ethylene glycol)(200)monomethacrylate (PEG(200)MA) was purchased from PolySciences (Warrington, PA, USA) and the heterobifunctional polyethylene glycol (PEG) derivative, acryloyl(polyethyleneglycol)-*N*-hydroxysuccinamide (MW 3500) (Acrl-PEG-NHS), was purchased from Jenkem Technology USA (Allen, TX, USA) or Nektar Therapeutics (Huntsville, AL, USA). The diacyrlate and methacrylate reagents were passed through an inhibitor removal column (Sigma-Aldrich, St. Louis, MO, USA) before use (for removal of hydroquinone and monomethyl ether hydroquinone polymerization inhibitors). Ferrocene monocarboxylic acid ($FcCO_2H$, 97%, Sigma-Aldrich) was used as received. A 0.1 M Tris buffer solution (adjusted to pH=7.2 using 1M HCl) was made from Tris(hydroxymethyl)aminomethane or Trizma® (99.8+%, A.C.S., Sigma-Aldrich). Trichloroethylene (spectrophotometric grade, ≥99.5%, Sigma-Aldrich), acetone (≥99.9%, Sigma-Aldrich), 2-propanol (≥99.8%, Sigma-Aldrich), ammonium hydroxide solution (ACS reagent, 28.0–30.0% as NH_3, Sigma-Aldrich), hydrogen peroxide solution (ACS reagent, 30 wt. % in H_2O, Sigma-Aldrich), ethanol (CHROMASOLV®, Sigma-Aldrich) and toluene (anhydrous, 99.8%, Across) were used as received. Cysteamine, 3-sulfopropyl methacrylate potassium salt and pyrrole (Py) monomer were obtained from Aldrich Chemical Co. (Milwaukee, WI, USA). The bi-functional monomer 2-methacryloyloxyethyl-4-(3-pyrrolyl)butanate (MPB) was synthesized in house.

2.1.2 Electrodes, electrochemical cell and instrumentation

Voltammetric experiments were performed using a three-electrode (working, counter and reference) electrochemical setup and were under the control of a BAS 100 Potentiostat/Galvanostat Electrochemical Analyzer equipped with a low current module and controlled by BAS 100 software (Bioanalytical Systems, West Lafayette, IN, USA). A platinum mesh was used as the auxiliary electrode. Gold micro-disc electrode arrays (MDEA 050 Au and ECC MDEA 5037 Au) and micro Ag|AgCl| 3M Cl^- electrodes were purchased from ABTECH Scientific, Inc. (Richmond, VA, USA) and used as the working and reference elec-

trodes, respectively. The MDEA electrodes were subject to cleaning, electrochemical polishing, chemical modification, functionalization, and derivatization before application of the hydrogel layer. Electrochemical impedance spectroscopic characterization of the hydrogel-coated or uncoated MDEA devices was performed using a 10 mV amplitude sine wave (0.1 Hz – 1 MHz; 25±1°C) obtained using Potentiostat/Galvanostat Model 283 (AMETEK Princeton Applied Research, Oakridge TN, USA) coupled with a Solartron 1260 Frequency Response Analyzer (FRA, AMETEK Solartron Analytical, Oakridge, TN, USA) linked to a Dell PC controlled by ZPlot software. The data was imported into MATLAB (The MathWorks, Inc, Natick, MA, USA) for analysis. Measurements of impedance changes of the poly (HEMA)-pyrrole gel with variable pH (6.1 to 8.8) were made using an electrochemical cell impedance analysis (EIA) system (single frequency measurement). For temporal electrical impedance analysis (EIA) of the hydrogel's electrical response to pH, the hydrogel formulations were cast in 8-well ECIS Cultureware™ Disposable Electrode Array (8W1E) chip (Applied Biophysics, Troy, New York, USA). The chips comprise eight (8) culture wells, each with a centrally located 250 μm diameter gold electrode exposed through hard-baked, Novalac® resist and a peripherally located, large area electrode at the base of each 5 ml well. The impedance measurement setup also included a computer for data acquisition and analysis, a Solartron 1260 frequency response analyzer (FRA), a Hewlett Packard relay box (HP 34970A Data Acquisition/Switch Unit) for multiplexing to the eight working electrodes of the 8W1E chips and a water-jacketed CO_2 incubator (VWR, West Chester, PA, USA) set to a temperature of 37°C at a relative humidity of 90–100% and CO_2 concentration of 5%. A chip holder (Applied Biophysics) served to provide an electrical interface between the 8W1E chips and the HP data acquisition unit.

2.2 Methods

2.2.1 MDEA cleaning and activation

Unpackaged MDEA 050-Au devices were cleaned by sequential ultrasonic washing in boiling trichloroethylene (3 min, 86.7°C), acetone (1 min; 56.2°C), 2-propanol (1 min; 82.4°C) and then washed profusely in room temperature (RT) deionized water. To remove residual organic/ionic contamination and to produce a uniform, reproducible layer of −OH groups on the surface of the Si_3N_4 (activation), the electrodes were immersed in a (5:1:1, *v/v/v*) 60°C solution of D.I. H_2O/NH_4OH/H_2O_2 (RCA Clean), held for 3 to 5 s, quenched in DI water for 1 min and then washed profusely with running DI water. Packaged MDEA 5037 devices were cleaned in 2-propanol (1 min; RT) and then washed profusely in room temperature deionized water. To remove adventitious chemisorbed organic residues, the MDEA 050-Au and MDEA 5037 devices were treated for 10 min in the UV-Ozone cleaner (UV_Clean, Boelkel Industries, PA, USA), washed by ultrasonication in 2-propanol and then washed profusely in room temperature deionized water.

2.2.2 MDEA surface modification and functionalization

The gold surface of the cleaned and activated MDEA devices was chemically modified with 0.01 M 3-mercapto-1-propanol (in anhydrous ethanol) and stored at room temperature overnight to introduce pendant alkylhydroxy surface functionalities. After modification, the MDEA 050 was rinsed by sequential ultrasonic washing for 1 min each in ethanol and an ethanol/toluene mixture (1:1, *v/v*) and finally in anhydrous toluene. The ECC MDEA 5037 was rinsed sequentially in ethanol, an ethanol/water mixture (1:1, *v/v*) and finally in DI water. This step served to remove non-chemisorbed (not attached) 3-mercapto-1-propanol molecules from the MDEAs. The pendant alkylhydroxy and surface −OH groups of the silicon nitride surface were subsequently functionalized by treatment with 3-(aminopropyl)trimethoxysilane (γ-APS; 0.01 M, in anhydrous toluene, RT, 2 h) in order to introduce pendant alkylamino surface functionalities. After alkylamino functionalization, the electrodes were rinsed by sequential washing for 1 min each in anhydrous toluene, then an ethanol/toluene mixture (1:1, *v/v*) and finally in anhydrous ethanol for the MDEA 050 and in an ethanol/water mixture (1:1, *v/v*) and anhydrous ethanol for the MDEA 5037. Finally, the MDEA devices were cured at 40°C for 20 min, then 110°C for 20 min, and then 40°C for 20 min, for a total of 1 h, in a 0.22-micron-filtered convection oven. The 250 μm gold electrodes of the 8W1E chip were each surrounded by an adhesive-backed silicone well of ID = 2.5 mm and depth = 2.0 mm which provided a volume of 9.82 μl around each electrode. The gold electrode and the surrounding Novalac® that were contained within the 2.5 mm diameter silicone well of the 8W1E chip were likewise chemically modified for attachment of the hydrogel layer. A solution of 0.01 M cysteamine in 0.05 M phosphate buffer solution (pH = 8.5) was placed within the well, covered, and incubated for 1 h at 37°C at 90–100% relative humidity. The Novalac® resin was modified by reaction with 3-aminopropyl-trimethoxysilane (0.1 wt.% in 10% ethanol) (16) by incubation for 1 h, then the wells were rinsed with DI water. For the final functionalization and to establish a continuous path of covalent bonding between the device surfaces and the hydrogel layer the MDEA devices and the 8W1E chip were incubated for 2 hours in Acrl-PEG-NHS

(MW=3500) solution (0.001 M) made up in 0.1 M HEPES (pH=8.5). Preparation of the Acrl-PEG-NHS solution and the derivatization step were performed in a UV filtered bioclean room or in the dark at room temperature. The modified devices were subsequently rinsed by ultrasonic washing for 1 min in DI water.

2.2.3 Formulation and fabrication of p(HEMA) hydrogel membranes

The hydrogel membrane was fashioned from a cocktail prepared by mixing HEMA, TEGDA, PEG(200)MA, HMMA and DMPA in a typical ratio 86:3:5:5:1 mol %. This mixture was then added to a 1:1 (*v/v*) solution of ethylene glycol/water so that the mixed solvent comprised 20 wt.%. Under UV-free conditions, the final hydrogel cocktail was sonicated, sparged with nitrogen gas and 20 μl of the hydrogel cocktail was applied evenly to the surface of the PEGylated (derivatized) MDEA 050. For the 8W1E chip, 2.5 μl of the hydrogel cocktail was added to the 2.5 mm diameter base of the cavity created by the silicone well. The mixture was immediately irradiated with UV light (366 nm, 2.3 W/cm^2, 5–7 min) in a UV cross-linker (CX-2000 CROSSLINKER, UVP, Upland, CA, USA) under an inert nitrogen atmosphere to effect polymerization of the hydrogel component. Packaged MDEA 5037 devices were similarly derivatized (PEGylated) but were dip coated. Finally, the electrodes were conditioned and un-reacted monomer extracted by sequential immersion in ethanol/deionized water mixtures (100% ethanol, 75:25; 50:50; 25:75; 100% DI water; *v/v*) for a minimum of 1 h each before being subjected to the next step. For the 8W1E chip, hydrogels were conditioned in 0.1 M Tris buffer with 0.1 M KCl at pH of 6.1 and allowed to incubate overnight at 37°C.

2.2.4 Cyclic voltammetry

Multiple scan rate cyclic voltammetry was performed using a three-electrode (working, counter and reference) electrochemical setup under the control of a BAS 100 Potentiostat/Galvanostat Electrochemical Analyzer, equipped with a low current module and controlled by BAS 100 software (Bioanalytical Systems, West Lafayette, IN, USA). A large surface area platinum gauze (3×2 in.) electrode (Alfa Aesar, USA) was used as the auxiliary electrode. Gold micro-disc electrode arrays (MDEA 050 Au and ECC MDEA 5037 Au) and Ag/AgCl electrodes were purchased from ABTECH Scientific, Inc. (Richmond, VA, USA) and used as the working and reference electrodes, respectively. The MDEA electrodes were subject to the cleaning protocol described above before electrochemical characterization. Voltammetry was performed by scanning over the potential range 0 to 600 mV at variable scan rates (10, 25, 50, 75, 100, 200, 250, 300, 400 and 500 mV/s). The working electrodes of the ECC MDEA 5037 (uncoated) and MDEA 050 (hydrogel coated and uncoated) were characterized by cyclic voltammetry at room temperature in solutions of 1 mM $FcCO_2H$ prepared in 0.1 M Tris/0.1 M potassium chloride (KCl; pH=7.2).

2.2.5 Capacitance determination by linear polarization resistance

The double layer capacitance, C_{dl}, of an electrified interface can be quantitatively approximated using the linear polarization resistance (LPR) technique wherein the potential of the working electrode is cycled over a very small potential range in an electrolyte without a redox-active (non-Faradic) constituent. Capacitance measurements were made on the un-coated and hydrogel-coated MDEA 050 Au as well as on the two separate (lactate sensing 1 and glucose sensing 2) working electrodes of the uncoated ECC MDEA 5037 chip (Table 1). Using the BAS 100 (low current module for the ECC MDEA 5037), MDEAs were scanned from 0.050–0.060 V (10 mV) at a scan rate, ν, of 0.01 V/s (10 mV/s) and the ensuing currents were sampled at 1 mV intervals. Measurements were made in 0.1 M TRIS buffer containing 0.1 M KCl.

Table 1 Specifications for the fabricated micro-disc arrays, where *r* is a radius of the individual microelectrodes on the array, *d,* is the centre-to-centre distance between micro-discs and *N* is the total number of microelectrodes making up the array

Working Electrodes	Number of discs (*N*)	Disc radius, *r*, (center to center distance, *d*; μm)	*d/r*	Active area (cm^2) (radius; cm)	Capacitance, C_{dl}	
					(nF)	(nF/cm^2)
MDEA 050	5,184	25 (100)	4	0.10 (0.1784)	4000±100(3)	40,000
MDEA 050 (hydrogel coated)	5,184	25 (100)	4	0.10 (0.1784)	2800±400(3)	28,000
MDEA 5037 (Distal, glucose sensing)	37	25 (100)	4	7.3×10^{-4} (0.0152)	30±1(3)	41,095
MDEA 5037 (Proximal, lactate sensing)	37	25 (100)	4	7.3×10^{-4} (0.0152)	31±1(3)	42,465

Mean capacitances for the uncoated and hydrogel-coated MDEA 050 and ECC MDEA 5037 (proximal and distal working electrodes) as determined from short range (50 mV to 60 mV), slow scan rate (10 mV/s) linear polarization resistance cyclic voltammograms.

2.2.6 Electrochemical impedance spectroscopy (EIS)

Two-electrode electrochemical impedance spectroscopy was performed using a Solartron Instruments Model 1260 Frequency Response Analyzer (FRA; Solartron Analytical, Hampshire, UK). In two-electrode mode, measurements were controlled by ZPlot impedance measurement software (Scribner Associates, Southern Pines, NC, USA). The impedance data was viewed in ZView (Scribner Associates) impedance plotting and visualization software. Impedance was measured between the working electrode of the MDEA 5037 or MDEA 050 and a large surface area platinum gauze (3×2 in.) counter electrode (Alfa Aesar, USA). The AC sine-wave excitation voltage amplitude was 10 mV, over the frequency range 0.1 Hz to 10 MHz. The probing electrolyte was 1.0 mM $FcCO_2H$ in a supporting electrolyte of 0.1 M TRIS buffer/0.1 M KCl (pH=7.2) solution at 20°C to various concentrations. Temporal impedance measurements of hydrogel pads were made in 0.1 M Tris buffer/0.1 M KCl solution at 37°C using a 50 mV p-t-p sine voltage at 4,000 Hz. Measurements were multiplexed to the 8 electrodes/wells of the 8W1E chip.

3 Results and discussion

3.1 Design and fabrication of MDEAs

Micro-disc electrode arrays (MDEAs) are single electrodes formed from a single contiguous layer of electrode material with electrolyte exposures that occur through an array of micron-dimensioned openings formed through an insulator. The geometric area of the exposed electrode is therefore divided amongst an array of micron-dimensioned electrodes (50 μm diameter) each connected one to the other but separated from the electrolyte by a passivating layer (0.5 μm thick) of silicon nitride (Si_3N_4). Figure 2 gives pictures and optical micrographs of the ECC MDEA 5037 device used in this work and show the hexagonal packing arrangements of the individual discs of the array. The working electrodes are thus hexagonal arrays of recessed microdiscs, fabricated by photolithographic techniques, with each micro-disc residing at the bottom of a cylindrical cavity etched through the Si_3N_4 passivation layer. The ECC MDEA 5037 is a dual electrochemical cell on a chip, with a large area counter electrode and reference electrode. However, these additional elements are not used in this work. Details of the micro-lithographic fabrication procedures are described elsewhere (Abdur Rahman 2008) while key specifications of the fabricated micro-disc arrays are presented in Table 1.

3.2 Capacitance measurements

Figure 3 shows typical voltammetric response of an un-coated and a hydrogel-coated micro-disc electrode array. The following equation was used to determine the double layer capacitance:

$$\frac{\Delta i}{2\upsilon} = C_{DL}$$

where Δi(A) is the difference between the oxidizing (more positive) and reducing (more negative) currents; υ is the scan rate (V/s) and C_{DL} (F) is the double layer capacitance.

The capacitance of the MDEA 050 working electrode was found to be 4.0±1.0 μF (n=3), while the capacitances of the ECC MDEA 5037 distal and proximal working electrodes were 30 nF (±1) and 31 nF (±1), respectively (Table 1). A student t-test (assuming independence and that they follow a normal distribution) of the paired working electrodes on the MDEA 5037 revealed that there is no significant difference between the mean capacitances of the distal and proximal electrodes (acceptance of the null hypothesis). The capacitance of an MDEA 050 electrode is expected to be about 100 times (two orders of magnitude)

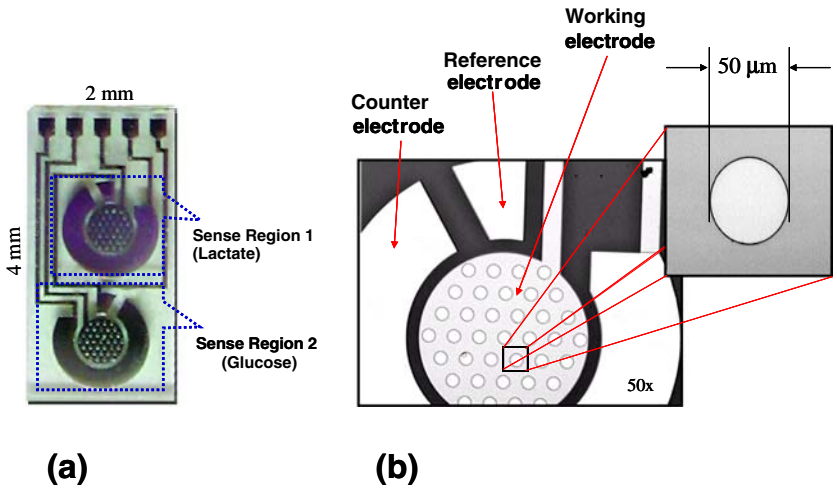

Fig. 2 (**a**) A picture of the ECC MDEA 5037 Au chip (**b**) An optical micrograph showing the three electrode electrochemical cell and the individual disc (insert) of the micro-disc array

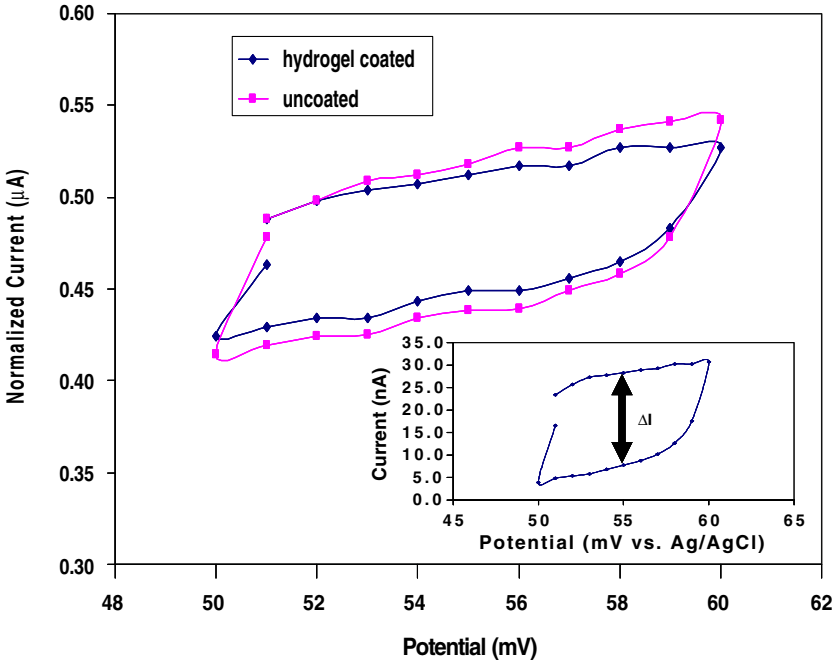

Fig. 3 The application of linear polarization resistance (LPR) technique to the determination of the double layer capacitance of MDEA 050 in the presence and absence of hydrogel layer. *Inset* LPR data of MDEA 5037 without hydrogel

larger than that of the MDEA 5037. Normalized on a per unit area basis (column 2) one notes that the capacitances are essentially the same confirming that the larger MDEA 050 is a suitable surrogate for the smaller MDEA 5037. The application of a hydrogel layer to the electrode surface produces two interfaces (or interphases): (1) an electrode-hydrogel interface; and (2) an hydrogel-solution interface. The addition of a new interface results in a dramatic impact on the impedance characteristics of the MDEA devices as well as on the diffusion of redox species (ferrocene mediator) to the microdisc gold working electrodes.

3.3 Cyclic voltammetric characterization

Cyclic voltammetry measurements of the model redox mediator, ferrocenecarboxylic acid, have been conducted to investigate the transport behavior of the un-coated and hydrogel-coated MDEAs. Figure 4 shows the cyclic voltammograms of the un-coated MDEA 050 Au (4a) and ECC MDEA 5037 (4b) devices obtained in 1.0 mM $FcCO_2H$ in a supporting electrolyte of 0.1 M TRIS buffer/0.1 M KCl (pH=7.2) solution at 20°C. Voltammograms were obtained over the range 0 to 600 mV and at scan rates that ranged

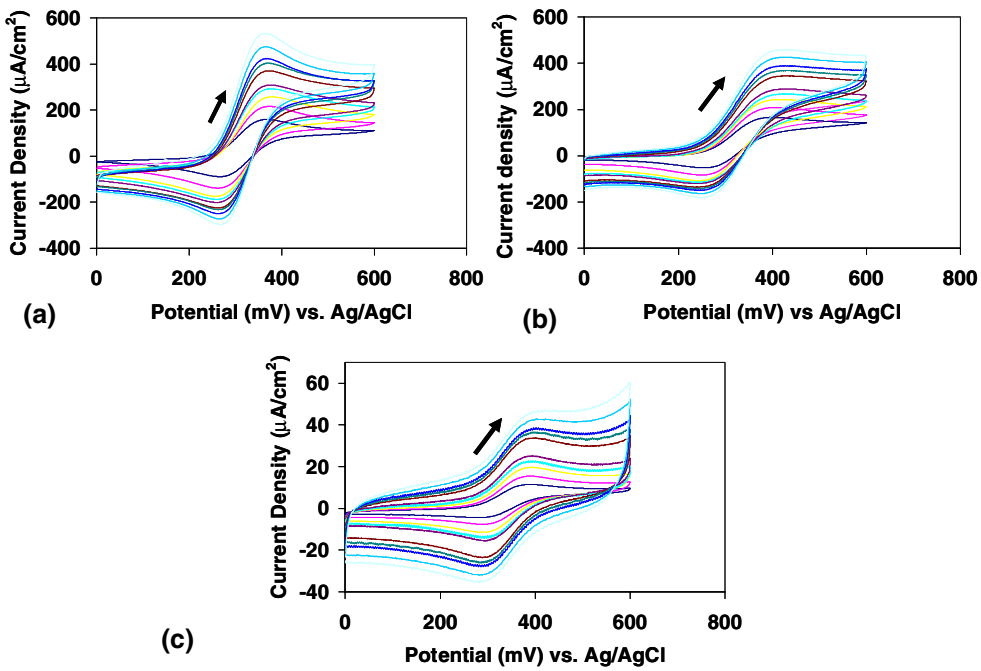

Fig. 4 Cyclic voltammograms recorded in aqueous 0.1 M TRIS buffer (pH=7.1) at 20°C containing 1.0 mM FcCO2H: (**a**) un-coated MDEA 050 Au, (**b**) un-coated ECC MDEA 5037 Au (**c**) hydrogel-coated MDEA 050 Au, B) hydrogel-coated ECC MDEA 5037 Au. Sweep rates were 10, 25, 50, 75, 100, 200, 250, 300, 400 and 500 mV/s

from 10 to 500 mV/s, specifically; 10, 25, 50, 75, 100, 200, 250, 300, 400 and 500 mV/s. Figure 4(c) shows the cyclic voltammograms of the hydrogel-coated MDEA 050 Au device obtained under similar test conditions.

Multiple scan rate cyclic voltammetry of the uncoated and hydrogel-coated MDEA devices in aqueous 0.1 mM $FcCO_2H$ revealed the expected quasi-reversible characteristics. The d/r=4 micro-discs produces the expected scan rate dependence associated with linear diffusion that transitions at higher scan rates but does not meet the expected scan rate independence associated with radial diffusion (Gonzalez-Garcia et al. 2007). Application of the poly(HEMA)-based hydrogel layer to the modified MDEA surface resulted in a significant decrease in the anodic and cathodic currents; falling by one order of magnitude without a change in ΔE_p.

One of the primary goals of this research is to develop a bioactive hydrogel layer that will improve tissue biocompatibility of the implanted device, stabilize the glucose oxidase and lactate oxidase enzymes within this sensing layer but also support facile analyte and mediator transport within the membrane. A consequence of the application of a hydrogel layer, however, may mean that sensitivity of the device is sacrificed. In spite of the lower sensitivities, the sigmoidal shape that characterizes the hydrogel-coated electrodes is an indication that there is adequate mass transport of the redox species to the electrode surface. The ratio i_{pa}/i_{pc} is a useful measure for determining whether a reaction is reversible, quasi-reversible or irreversible. For un-coated MDEA 050 devices this ratio is equal to 1.0, confirming the reversibility of the ferrocene ⇔ ferrocenium couple. However, for the poly(HEMA)-based hydrogel-coated MDEA 050 device this ratio is 1.3 suggesting that the presence of the hydrogel layer favors the ferrocene to ferrocenium reaction over the disappearance of ferrocenium species of the now quasi-reversible reaction. Reversible, one-electron, charge-transfer reactions such as the ferrocene to ferrocenium reaction are identified by the fact that their peak separation potential, ΔE_p, is given by $\frac{0.0592}{n}$ V. In all cases, the measured values of ΔE_p were greater than 90 mV (0.09 V) indicating quasi-reversibility.

From the voltammograms illustrated in Fig. 4(a) and (b), there are clearly evident differences in the shape of the voltammograms that manifests in the ratio of the anodic to the cathodic peak current. For the uncoated MDEA 050 Au, the ratio, i_{pa}/i_{pc}, was found to be equal to unity for almost all scan rates. However, this ratio was slightly greater for the uncoated ECC MDEA 5037 which was 1.3. Also, at lower scan rates, there is also evidence of increasing microelectrode behavior as the voltammograms move from the characteristic shape typical of reversible reactions at planar electrodes experiencing semi-infinite linear diffusion to the sigmoidal shape characteristic of electrodes possessing micron sized dimensions and experiencing radial diffusion. By comparison, the smaller MDEA 5037, in addition to the smaller peak currents, exhibits sigmoidal voltammograms that are indicative of their working electrode geometries. The shapes of the voltammograms are therefore influenced not only by the size of he discs and inter-disc spacing but by the number density of discs in the array.

Coating of the MDEA 050 with a hydrogel layer results in an appreciable attenuation in the anodic and cathodic current density; by approximately one full order of magnitude. This is the result of the reduced apparent diffusion coefficient of ferrocenecarboxylic acid within the hydrogel layer. CV of the MDEA 050 device revealed a reduction in the apparent diffusion coefficient of ferrocenemonocarboxylic acid ($FcCO_2H$), from 6.68×10^{-5} to 6.74×10^{-6} cm^2/s for the uncoated and 6 μm thick hydrogel coated devices, respectively. Randles–Sevcik plots of peak current versus the square root of scan rate (I_p *vs.* $v^{1/2}$) generally reveal useful insight regarding the relationship between diffusion properties and electrode area of an electrochemical system under linear diffusion conditions (Bard and Faulkner 2001). Figure 5 illustrates the Randles–Sevcik type plots expressed in current densities (for both anodic and cathodic peak currents) for the un-coated and hydrogel-coated MDEA 050 and the un-coated ECC MDEA 5037 devices. Despite the large differences in overall area and the large differences in the number of 50 μm diameter discs (5,184 *vs.* 37) the overall current densities are shown to be quite similar. It is also immediately clear that the curves, as a whole, are non-linear with transitional characteristics where the slopes of the curves suddenly change at a critical scan rate.

A simulation of the cyclic voltammograms produced by MDEAs and reported by Saito (1968) shows that the ratio of d/r is a key parameter which could be used to define the two principal diffusion domains. The transport domain of independent micro-disc electrode behavior is characterized by $R_0/r>6$, i.e. $d/r>12$, where $2R_0=d$. For the two MDEA devices of this work, the d/r = 4, which are expected to produce cyclic voltammograms that are peak-shaped (linear diffusion). Figure 5(a) (un-coated MDEA 050 Au) shows two characteristic limiting polarization curves: (1) sigmoidal-shaped voltammograms that relate to spherical diffusion at lower scan rates, and (2) peak-shaped voltammograms that correspond to reversible linear diffusion at higher scan rates. This confirms that over the scan rates investigated, there is no defined diffusion characteristic of the system.

3.4 Impedance measurements

3.4.1 EIS analysis of MDEAs

AC impedance measurements were performed on the hydrogel coated MDEA 050. Figure 6 is the Bode diagram

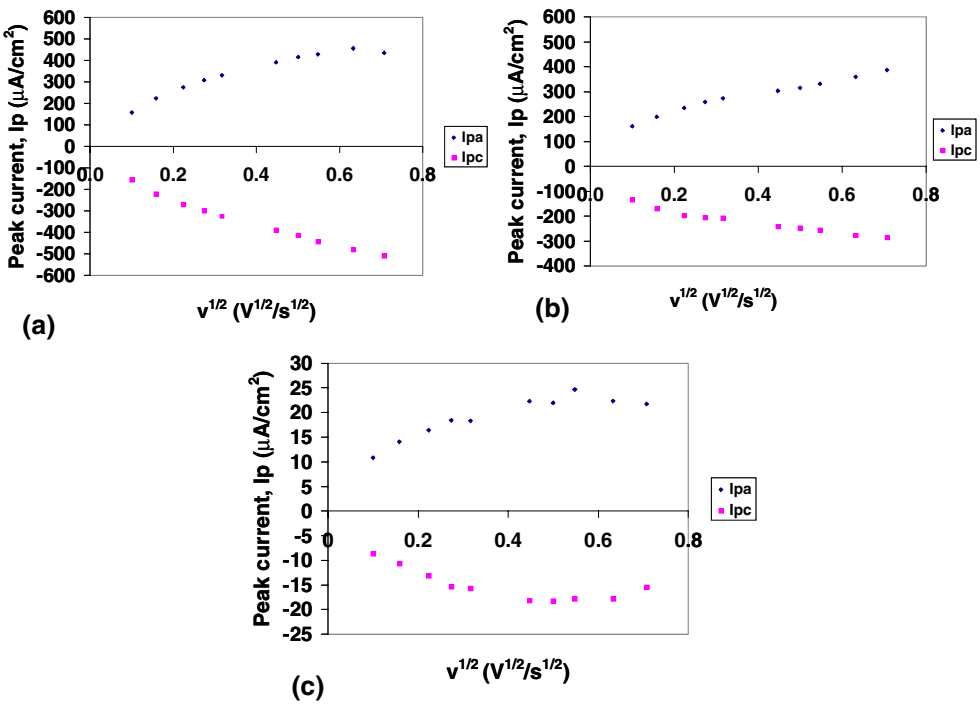

Fig. 5 Randles–Sevcik plots for (**a**) un-coated MDEA 050 Au, (**b**) un-coated ECC MDEA 5037 Au (**c**) hydrogel-coated MDEA 050 Au, (**b**) hydrogel-coated ECC MDEA 5037 Au. Sweep rates were 10, 25, 50, 75, 100, 200, 250, 300, 400 and 500 mV/s

of the MDEA 050 chip with and without the hydrogel coating in 1 mM $FcCO_2H$ in 0.1 M Tris/0.1 M KCl. In the absence of the hydrogel layer, the impedance of the MDEA 050 device exhibits charge transfer and double layer characteristics as evidenced by the impedance phase angle tending towards resistive behavior at low frequencies. The impedance data of the MDEA 050 in the absence of the hydrogel layer was modeled using a classical Randles equivalent circuit with a constant phase element (CPE) representing diffusion. This circuit fits the data very well with a fit standard deviation of 0.0004. In the presence of the hydrogel layer on the MDEA 050 chip, the impedance was considerably increased. The impedance data of the hydrogel-coated MDEA 050 device was parameterized with a classical Randles circuit but without a constant phase element (CPE) representing diffusion. The model fits the data very well with a fit standard deviation of 0.002. The inclusion of the diffusion element lead to poorer estimates of diffusion parameters indicating that the inclusion of a constant phase element (CPE) representing diffusion was not necessary in the parameterization of the data. This does not negate the contribution of diffusion but simply informs that the effect of diffusion is not observed within the EIS interrogation frequency range 0.1 Hz to 10 kHz.

The MDEA 5037 is equipped with two working electrodes that are scaled versions of the MDEA 050 electrode.

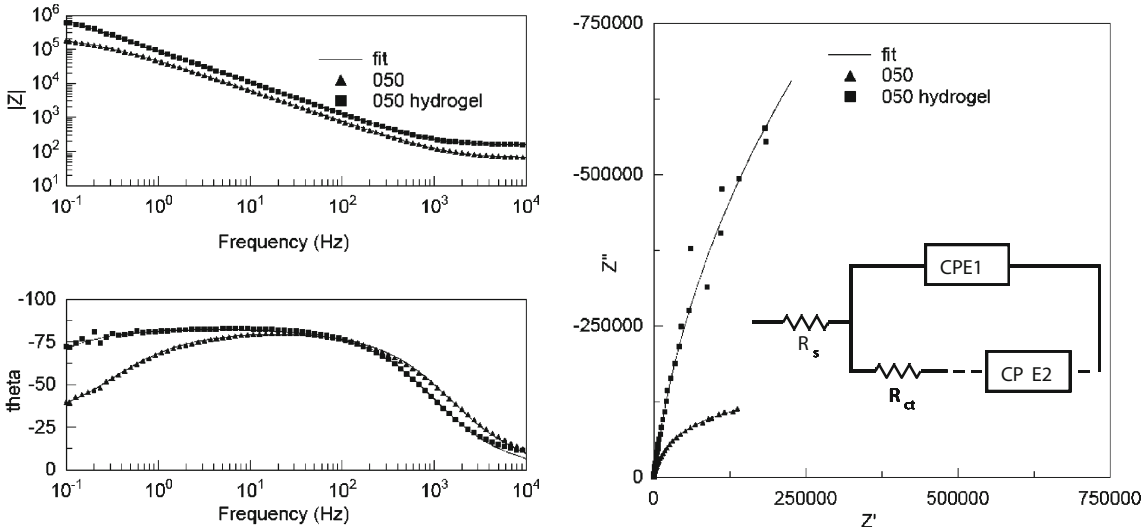

Fig. 6 Bode plot, phase angle plot and Cole–Cole plot comparing uncoated and hydrogel coated MDEA 050

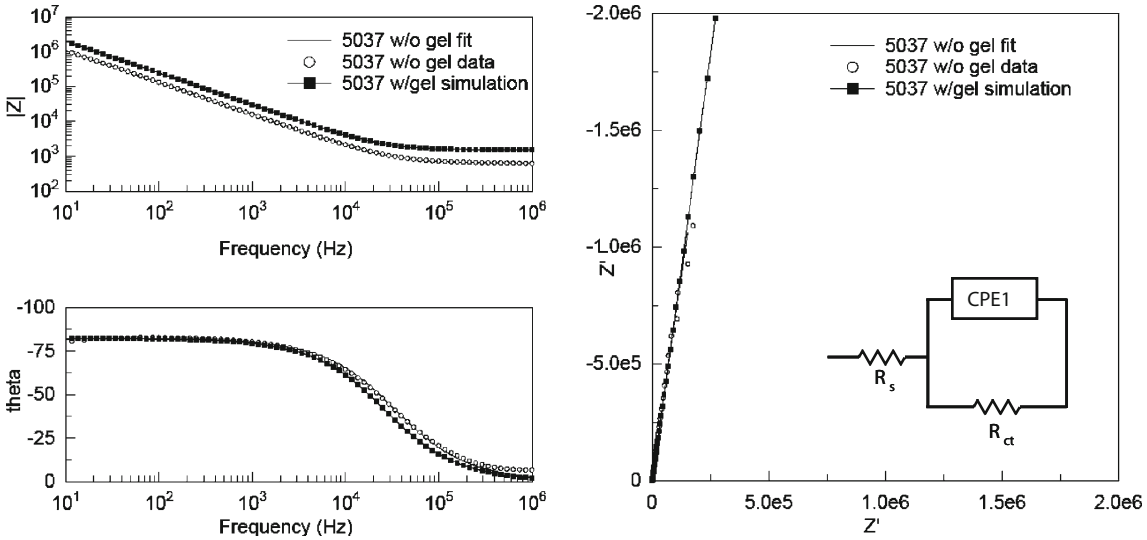

Fig. 7 Bode plot, phase angle plot and Cole–Cole plot comparing uncoated and hydrogel coated MDEA 5037. The hydrogel coated MDEA 5037 results are predicted based on the establishment of a theoretical model from simulations derived from the coated and uncoated MDEA 050 measurements

Due to the reduced surface area (7.3×10^{-4}cm^2 for the MDEA 5037 compared to 0.1 cm^2 for the MDEA 050), the MDEA 5037 chip has a very high impedance. With the application of the hydrogel layer to the MDEA 5037, the impedance is expected to be even higher based on projections from the hydrogel-coated MDEA 050 impedance study. Figure 7 is the bode diagram of uncoated MDEA 5037 in 1.0 mM $FcCO_2H$ in 0.1 M Tris and 0.1 M KCl. The electrode impedances scale very well with the surface area of the electrode as was previously demonstrated by (Abdur Rahman 2008). The difference in the absolute impedance between the MDEA 050 and 5037 is approximately two orders of magnitude, which is consistent with the difference between the electroactive surface areas of the two chips.

Based on circuit models previously established comprising resistive and CPE elements (Abdur Rahman 2008), one can arrive at theoretical values for Rsp, Q, n and Rct for the hydrogel coated MDEA 5037 (Table 2). An increase in both the spreading and charge transfer resistances are expected as a result of deposition of the hydrogel layer onto the ECC MDEA 5037 device. A decrease, however, in the Q value of the CPE element is expected.

3.4.2 Impedimetric study of pH variability using EIA

Time dependent impedance measurements were performed on hydrogels at a frequency of 4 kHz and a sinusoidal peak-to-peak potential of 50 mV. Figure 8 shows the 8-well culture ware and the adhesive backed silicone levees that were used to contain the hydrogel formulation and create gel pads. Measurements were made on the hydrogels within each of the culture wells when 0.1 M Tris buffer (with 0.1 M KCl) solution of variable pH values (adjusted to 6.1, 7.2 and 8.8 using 1 M hydrochloric acid) were pipetted into the wells. Clear and distinguishable impedance responses (lighter plots) to the changing pH values were observed (Fig. 9). When the pH was adjusted initially from 6.1 to 7.2, all the wells consistently responded with a decrease by approximately 5% in the real impedance. At t=400 min a different pH adjustment was made for each of the wells. Wells 3–4 remained at pH 7.2, and as can be seen from Fig. 9, the impedance did not change, but rather continued its gentle decline along the same path. The slight increase in impedance initially for these two unchanged wells was due to opening of the incubator door which affected not only the temperature, but also humidity within the

Table 2 Comparison of the impedance properties of uncoated and hydrogel coated MDEA devices based on a CPE model

Microdisc electrode arrays	CPE			
	Rsp (Ω)	Q (S.sn)	N	Rct (Ω)
MDEA 050	64.37	3.90	0.90	1.76×10^5
Hydrogel coated MDEA 050	152.5	2.11	0.91	3.35×10^6
MDEA 5037	630	0.021	0.91	1.57×10^8
Hydrogel coated MDEA 5037	1492.5 (predicted)	0.011 (predicted)	0.91 (predicted)	4.05×10^9 (predicted)

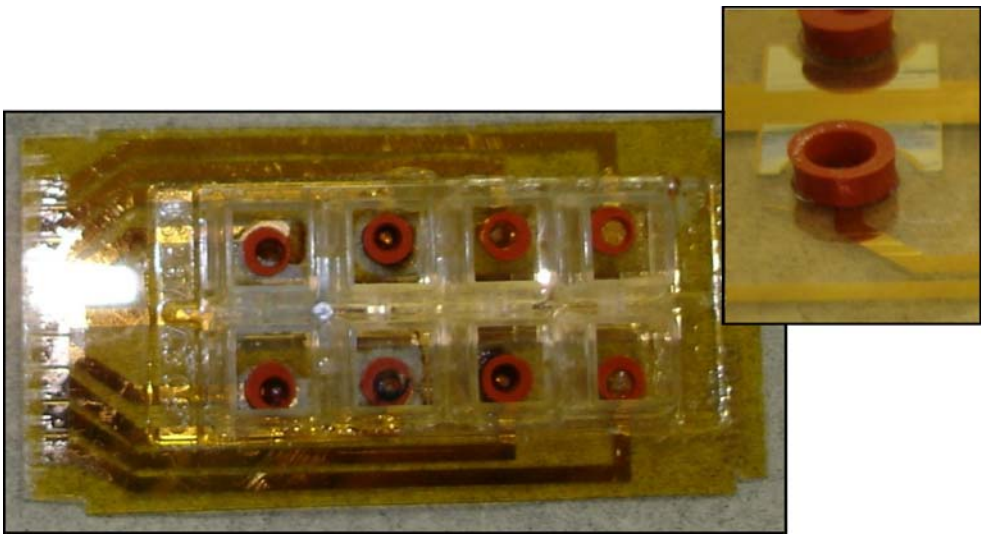

Fig. 8 Normalized real impedance of chip showing the pH response of the hydrogels. *Lighter* (*pastel*) *colors* are from the first set of impedance measurements, while the *darker* (*bold*) *colors* illustrate measurements performed a week later to demonstrate repeatability. The *dashed line* shows how the two different runs match up by taking into account the drift

incubator. Wells 5–6 at t=400 min, were returned to a pH of 6.1 at which point, the real impedance returned to their initial levels. This demonstrates clearly that the hydrogels respond in a reversible manner to variations in pH. Such a reversible response lies at the very heart of a biomedical device. Wells 7–8 at t=400 min, were increased further to pH 8.8 which results in the real impedance further dropping by about 20% of the initial value (at t=0 min). As can be seen in Fig. 9, each of the pH changes can clearly be differentiated by the changes in the impedimetric responses. Another important and necessary feature of the hydrogels is repeatability of their responses to pH changes. Fig. 9 also shows with another run of the same chip where the pH is changed from 6.1 to 8.8 pH (darker plots). The impedance response to the increase in pH matched up almost exactly with the measurements made a week earlier thereby establishing the repeatability of the pH response of the hydrogels.

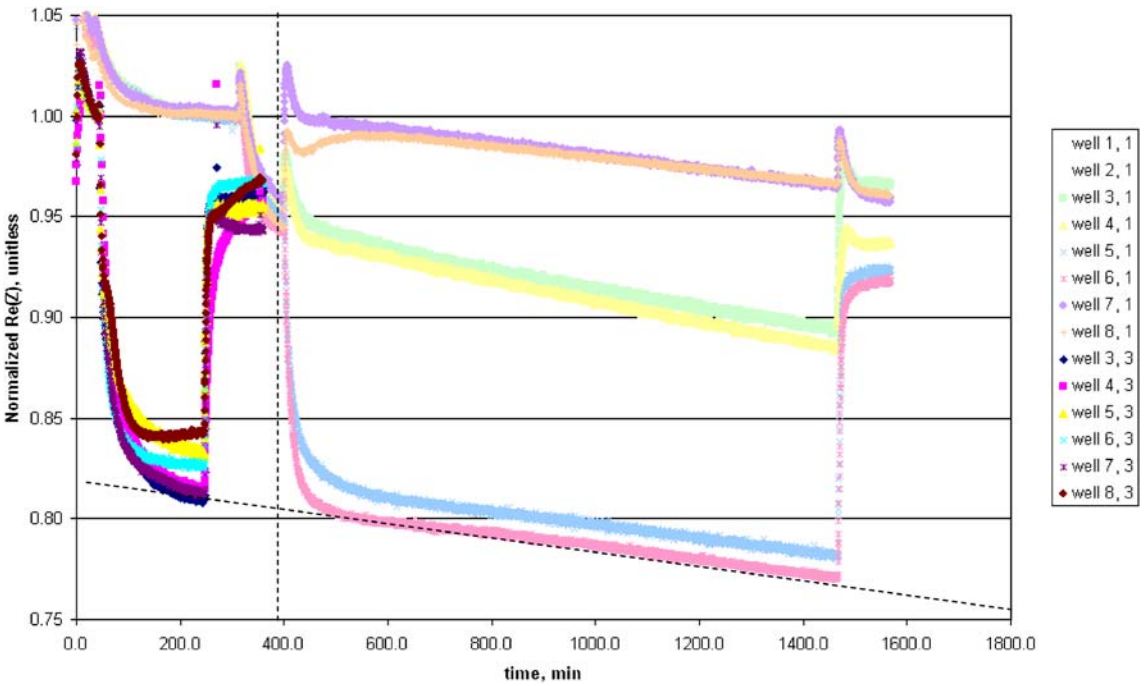

Fig. 9 Plots of normalized real component of the impedance acquired from an 8W1E chip showing the pH response of the hydrogels. The *bold colored plots* represent impedance measurements made a week following those represented by the *pastel colors* in the background. The *dashed line* demonstrates how the two different runs match up, taking into account the drift, and therefore, highlights the repeatability of the measurements

4 Conclusions

Modification of the MDEA 050 surface through the application of a hydrogel layer decreases the diffusivity of ions and redox species to and from the electrode-hydrogel interface, resulting in smaller current densities. Although the hydrogel will serve to improve the biocompatibility of the device, as well as support stability of immobilized enzyme activity for extended periods of time, overall current will be sacrificed. An important goal would therefore be to adjust the compositions of the hydrogel layer to confer the desirable properties of high diffusion coefficient, in addition to the aforementioned characteristics of biocompatibility and support of enzyme stability. This necessitates engineering the crosslink density, nanoporous structure and optimizing the relationship between enzyme loading with thickness to support maximum substrate and mediator flux. The MDEA 050 and the smaller MDEA 5037 demonstrate clear scaling characteristics with respect to double layer capacitance (determined by LPR technique).

For the MDEA 050 device, application of the hydrogel layer results in an increase in impedance (and consequently decrease in current density) that can be correlated to the reduced diffusivity of the redox species through the hydrogel layer and an increase in the charge transfer resistance, Rct and the spreading resistance, Rsp. A decrease in the double layer capacitance, associated with an increase in the complex impedance plane $(j\times\omega\times C)^{-1}$, is also apparent with the application of the hydrogel layer to the MDEA 050. The poly(HEMA) hydrogels containing interpenetrating polypyrrole demonstrated a significant, repeatable, and consistent response to step-changes in pH. Increasing pH from 6.1 to 7.2 and the subsequently up to 8.8 resulted in a decrease in the real impedance by up to 20% of the initial values (at pH 6.1).

Funding This work was supported by the US Department of Defense (DoDPRMRP) grant PR023081/DAMD17-03-1-0172 and by the Consortium of the Clemson University Center for Bioelectronics, Biosensors and Biochips (C3B).

References

Abdur Rub Abdur Rahman, Gusphyl Justin and Anthony Guiseppi-Elie "Towards an Implantable Biochip for Glucose and Lactate Monitoring using Micro-Disc Electrode Arrays (MDEAs)" "*Biomedical Microdevices: BioMEMS and Biomedical NanoTechnology"* (this journal)

S. Abraham, S. Brahim, K. Ishihara, A. Guiseppi-Elie, Molecularly engineered p(HEMA)-based hydrogels for implant biochip biocompatibility Biomaterials **26**, 4767–4778 (2005). doi:10.1016/j.biomaterials.2005.01.031

A.J. Bard, L.R. Faulkner, *Electrochemical Methods: Fundamentals and Applications*, 2nd edn. (John Wiley and Sons, Inc., Hoboken, 2001)

U. Bhardwaj, R. Sura, F. Papadimitrakopoulos, D.J. Burgess, Controlling acute inflammation with fast releasing dexamethasone-PLGA microsphere/PVA hydrogel composites for implantable devices J. Diabetes Sci. Technol. **1**, 8–17 (2007)

R. Compton, A. Fisher, R.G. Wellington, P.J. Dobson, P.A. Leigh, Hydrodynamic voltammetry with microelectrodes. cannel microband electrodes: theory and experiment J. Phys. Chem **97**, 10410–10415 (1993). doi:10.1021/j100142a024

T. Davies, R. Compton, The cyclic and linear sweep voltammetry of regular and random arrays of microdisc electrodes: Theory J. Electroanal. Chem **585**, 63–82 (2005). doi:10.1016/j.jelechem.2005.07.022

T. Davies, S. Ward-Jones, C. Banks, J. del Campo, R. Mas, F.X. Munoz et al., The cyclic and linear sweep voltammetry of regular arrays of microdisc electrodes: Fitting of experimental data J. Electroanal. Chem **585**, 51–62 (2005). doi:10.1016/j.jelechem.2005.07.021

R.H. Farahi, R.H. Farahi, T.L. Ferrell, A. Guiseppi-Elie, P.A.H.P. Hansen, "Integrated electronics platforms for wireless implantable biosensors" presented at Life Science Systems and Applications Workshop, 2007. LISA 2007. IEEE/NIH, 2007

H.O. Finklea, D.A. Snider, J. Fedyk, E. Sabatani, Y. Gafni, I. Rubinstein, Characterization of octadecanethiol-coated gold electrodes as microarray electrodes by cyclic voltammetry and ac impedance spectroscopy Langmuir **19**, 3660–3667 (1993). doi:10.1021/la00036a050

M. Gerritsen, A. Kros, V. Sprakel, J. Lutterman, R. Nolte, J. Jansen, Biocompatibility evaluation of sol-gel coatings for subcutaneously implantable glucose sensors Biomaterials **21**, 71–78 (2000). doi:10.1016/S0142-9612(99)00136-2

R. Gifford, J. Kehoe, S. Barnes, B. Kornilayev, M. Alterman, G. Wilson, Protein interactions with subcutaneously implanted biosensors Biomaterials **27**, 2587–2598 (2006). doi:10.1016/j.biomaterials.2005.11.033

O. Gonzalez-Garcia, C. Arino, J. Diaz-Cruz, M. Esteban, Chronoamperometric and voltammetric characterization of gold ultramicroelectrode arrays Electroanalysis **19**, 429–435 (2007). doi:10.1002/elan.200603727

A. Guiseppi-Elie, S. Brahim, G. Slaughter, K. Ward, Design of a subcutaneous implantable biochip for monitoring of glucose and lactate IEEE Sens. J. **5**, 345–355 (2005). doi:10.1109/JSEN.2005.846173

F.J. Holly, M.F. Refojo, Wettability of hydrogels I. Poly(2-hydroxyethyl methacrylate) J. Biomed. Mater. Res **9**, 315–326 (1975). doi:10.1002/jbm.820090307

H.J. Lee, C. Beriet, R. Ferrigno, H. Girault, Cyclic voltammetry at a regular microdisc electrode array J. Electroanal. Chem **502**, 138–145 (2001). doi:10.1016/S0022-0728(01)00343-6

M. Morita, M. Longmire, R.W. Murray, Solid-state voltammetry in a three electrode electrochemical cell-on-a-chip with a microlithographically defined microelectrode Anal. Chem **60**, 2770–2775 (1988). doi:10.1021/ac00175a026

M. Morita, O. Niwa, T. Horiuchi, Interdigitated array microelectrodes as electrochemical sensors. Electrochim. Acta **42**, 3177–3183 (1997). doi:10.1016/S0013-4686(97)00171-0

I. Moser, G. Jobst, G. Urban, Biosensor arrays for simultaneous measurement of glucose, lactate, glutamate and glutamine Biosens. Bioelectron. **17**, 297–302 (2002). doi:10.1016/S0956-5663(01)00298-6

F. Moussy, D. Harrison, D. O'Brien, R. Rajotte, Performance of subcutaneously implanted needle-type glucose sensors employing

a novel trilayer coating Anal. Chem. **65**, 2072–2077 (1993). doi:10.1021/ac00063a023

F. Moussy, D. Harrison, R. Rajotte, A miniaturized Nafion-based glucose sensor: in vivo evaluation in dogs Int. J. Artif. Organs **17**, 88–94 (1994)

L. Murphy, Biosensors and bioelectrochemistry Curr. Opin. Chem. Biol. **10**, 177–184 (2006). doi:10.1016/j.cbpa.2006.02.023

R.S. Nicholson, I. Shain, Theory of stationary electrode polarography: Single scan and cyclic methods applied to reversible, irreversible, and kinetic systems Anal. Chem **36**, 706–723 (1964). doi:10.1021/ac60210a007

J. Pickup, D. Claremont, G. Shaw, Responses and calibration of amperometric glucose sensors implanted in the subcutaneous tissue of man Acta Diabetol. **30**, 143–148 (1993). doi:10.1007/BF00572858

Y. Saito, Rev Polarog (Japan), vol. 15, pp. 177 (1968)

O. Schuvailo, O. Soldatkin, A. Lefebvre, R. Cespuglio, and A. Soldatkin, Highly selective microbiosensors for in vivo measurement of glucose, lactate and glutamate. Analytica Chimica Acta, vol. Epub 110-6, pp. 573–574, (2006)

A. Steinschaden, D. Adamovic, G. Jobst, R. Glatz, G. Urban, Miniaturised thin film conductometric biosensors with high dynamic range and high sensitivity Sens. Actuators B Chem **44**, 365–369 (1997). doi:10.1016/S0925-4005(97)00227-X

J. Vincent, Lactate and biochemical indexes of oxygenation, in Principles and Practice of Intensive Care Monitoring, ed. by M. Tobin (McGraw-Hill, New York, 1998)

K. Ward, R. Ivatury, R. Barbee, Endpoints of resuscitation for the victim of trauma J. Intensive Care Med. **16**, 55–75 (2001). doi:10.1046/j.1525-1489.2001.00055.x

W. Ward, J. Jouse, J. Birck, E. Anderson, L. Jansen, A wire-based dual-analyte sensor for glucose and lactate: in vitro and in vivo evaluation Diabetes Technol. Ther. **6**, 389–401 (2004). doi:10.1089/152091504774198106

G. Wilson, R. Gifford, Biosensors for real-time in vivo measurements Biosens. Bioelectron **20**, 2388–2403 (2005). doi:10.1016/j.bios.2004.12.003

B. Yu, Y. Ju, Y. Moussy, F. Moussy, An investigation of long-term performance of minimally invasive glucose biosensors Diabetes Technol. Ther. **9**, 265–275 (2007). doi:10.1089/dia.2006.0020